Expansion of the spectral representation function of a composite material in a basis of Legendre polynomials: Experimental determination and analytic approximations

C. Pecharromán[1] and F. J. Gordillo-Vázquez[2]
[1]*Instituto de Materiales de Madrid, C.S.I.C., Cantoblanco, 28049 Madrid, Spain*
[2]*Instituto de Óptica, C.S.I.C, Serrano 121, 28006 Madrid, Spain*
(Received 2 February 2006; revised manuscript received 24 April 2006; published 31 July 2006)

A unique formulation is presented to derive the spectral representation function of heterogeneous two-component materials in terms of an expansion on Legendre polynomials. This approach notably simplifies the calculations needed to estimate the effective dielectric function from the spectral density function and allows one to extract it from experimental data by using quite simple analytic expressions. The spectral representation function derived by the present method agrees notably well with experimental infrared reflectance measurements obtained from several ionic compounds. In addition, we state that the infrared spectral region is the optimal one in order to determine the full relationship between the spectral density function and the effective dielectric constant of a composite material.

DOI: 10.1103/PhysRevB.74.035120 PACS number(s): 77.22.−d, 02.70.Hm, 07.05.Kf, 05.10.Ln

I. INTRODUCTION

The precise determination of the electrical and optical properties of heterogeneous materials is still a challenging problem, although the basic physical laws describing these aggregates are the well-known Maxwell equations. In the case that we restrict the study to particles smaller than the light wavelength in vacuum, only the Laplace equation, with adequate boundary conditions, is needed to fully describe the problem. However, in spite of this apparent simplification, in realistic heterogeneous materials composed of submicrometric particles, a precise geometrical description of the material system is rarely possible.[1]

In order to approach the solution of the Laplace equation, several authors have used an expansion of the potential function in Legendre polynomials around the center of each of the particles making up the composite.[2] Additionally, many models have been developed based on some of the few cases for which the Laplace equation admits an analytical and relatively simple solution. The most widely known of them is that of an ellipsoid embedded in an infinite region of constant electric field. Based on this fact, several theories have been put forward as, for example, that of Maxwell-Garnett,[3] the effective medium theory,[4,5] Landau,[6] and others.[7,8] From these methods, the effective medium theory has shown to be the most flexible and able to approximately reproduce many of the available experimental results.[9]

The above-mentioned theories can all be obtained as particular cases of the so-called spectral representation method of the effective dielectric constant.[10,11] This method states that the effective dielectric constant of a heterogeneous material can be written as a function of the ratio of the dielectric constant of one of the composite phases to that of the other, and in terms of a geometrical function, the so-called spectral density function, $g(n)$ (where n runs from 0 to 1 and it stands for the depolarization factor of the particles making up the composite). This function is determined by the shape and distribution of the interfaces between the different phases present in the composite. Moreover, this function is constrained by a number of sum rules.[12,13] A considerable number of theoretical and empirical models[14–21] of $g(n)$ have been described in the literature that fit reasonably well to experimental data.

Several works have exposed different procedures to deduce the spectral density function from experimental infrared (IR) reflectance data without assuming a previous model for the spectral density function. These approaches estimate $g(n)$ by using a Monte Carlo algorithm,[22] by a continuous fraction,[23] a least squares fitting procedure,[24] or by a combination of them.[25] According to some of the authors of these works,[22] the process to extract $g(n)$ from experimental data of $\langle\varepsilon\rangle$ is ill posed, so that small errors in $\langle\varepsilon\rangle$ could carry large mistakes in $g(n)$. In all cases, models discretize the spectral representation function in small intervals where it is assumed that the function takes constant values. Thus, the higher the precision of the fitted values, the narrower the interval considered. However, in order to minimize the impact of the experimental data on the spectral representation function, constrictions given by sum rules must be incorporated into the calculations. Additionally, Tuncer[25] has introduced a more robust formalism, previously applied to the estimation of inversion of dielectric relaxation spectra,[26,27] based on the random selection (by a Monte Carlo technique) of the n intervals. These processes notably complicate the determination of $g(n)$ in such a way that it is very difficult to reproduce the calculations without a deep knowledge of computer programming.

In the present paper we introduce a unique formulation, based on an expansion on Legendre polynomials, to extract $g(n)$ from experimental measurements. This method notably simplifies most of the calculations needed to estimate $\langle\varepsilon\rangle$ from $g(n)$. In addition, our procedure automatically provides, by using quite simple expressions, the needed constraints in order to determine the spectral density function from experimental data. The spectral density functions determined by this method agree significantly well with experimental results. Moreover, a simple and fully analytical expression for $\langle\varepsilon\rangle$, which only depends on the filling factors and the percolation strengths, can be deduced.

In order to determine $g(n)$ from spectroscopic experiments, we have used the property that relates a surface plasmon resonance of the experimental spectrum to the condition

$$(1-n)\varepsilon_m + n\varepsilon_p = 0. \tag{1}$$

When this condition is satisfied, a peak at the absorbance and a band at the reflectance spectra appear. Since n runs from 0 to 1, we would get a set of resonances, corresponding to all values of n, with a weight related to $g(n)$ only if ε_p runs from $-\infty$ to 0. While metallic materials satisfy this condition all along the spectral range (more than 14 frequency orders of magnitude), a very unique narrow spectral area, called the reststrahlung region, exists in strongly ionic dielectric materials, where the complex dielectric function exhibits a resonance in such a way that it takes values all along the upper complex semiplane. In particular, the real part takes large negative values close to ω_T, i.e., the transverse phonon frequency ($\varepsilon_p \sim -100$) to reach the null value, $\varepsilon_p = 0$, at ω_L, i.e., the longitudinal phonon frequency. The larger the longitudinal-transverse splitting is, the more negative ε_p becomes. Typically, the largest ω_T-ω_L splitting is around 500 cm^{-1} wide, a spectral region that can be easily measured by a single IR spectrum. In this sense, the best materials that exhibit this property are ferroelectrics or strongly ionic materials (MgO, alkaline halides, etc.).

II. THEORETICAL APPROACH

The spectral representation theory states that the effective dielectric constant $\langle\varepsilon\rangle$ of a heterogeneous medium made up of two phases, labeled p and m, with dielectric functions ε_p and ε_m and filling fractions $f_p = f$ and $f_m = 1-f$, is given, according to the notation of the Fuchs and Claro paper,[14] by

$$\frac{\langle\varepsilon\rangle}{\varepsilon_m} - 1 = f\left[C_p\left(\frac{\varepsilon_p}{\varepsilon_m} - 1\right) + \int_0^1 \frac{g_p(n)}{\dfrac{\varepsilon_m}{\varepsilon_p - \varepsilon_m} + n} dn\right], \tag{2}$$

where $g_p(n)$ is the spectral density function for phase p, C_p is the so-called percolation strength of phase p, and n can be identified as the depolarization factor. In general, $g_p(n)$ is a complicated function of the geometric structure of the composite.

We can rewrite expression (2) as

$$\frac{\langle\varepsilon\rangle}{\varepsilon_m} - 1 = f\left[C\left(\frac{\varepsilon_p}{\varepsilon_m} - 1\right) + \int_0^1 \frac{g(n)}{\dfrac{\varepsilon_m}{\varepsilon_p - \varepsilon_m} + n} dn\right]. \tag{3}$$

This expression can be easily converted into a Hilbert transform by introducing two new variables. In the first place, we adopt the following change of variable:

$$x = 1 - 2n; \tag{4}$$

the second new variable τ is defined as

$$\tau = \frac{2\varepsilon_m}{\varepsilon_p - \varepsilon_m} + 1 = \frac{\varepsilon_p + \varepsilon_m}{\varepsilon_p - \varepsilon_m}. \tag{5}$$

The variable τ relates the dielectric constants ε_p and ε_m of the two components of the composite. After some algebra, we can derive the relationship between ε_p and ε_m from expression (5) and we have

$$\varepsilon_p = \varepsilon_m\left[\frac{\tau+1}{\tau-1}\right] \Rightarrow \begin{cases} \varepsilon_p(\tau=-1) = 0 \\ \varepsilon_p(\tau=1) = -\infty \end{cases}. \tag{6}$$

Thus, the variable τ belongs to the interval $\tau \in [-1,1]$.

Introducing Eqs. (4) and (5) into (2) and (3), the effective dielectric constant can be written as the Hilbert transform of the spectral representation functions of the p or m medium, respectively, as follows:

$$\langle\varepsilon\rangle = \varepsilon_m + fC_p(\varepsilon_p - \varepsilon_m) + \frac{f\varepsilon_m}{2}\int_{-1}^{1} \frac{g_p(x)}{\tau - x} dx, \tag{7}$$

$$\langle\varepsilon\rangle = \varepsilon_p + (1-f)C_m(\varepsilon_m - \varepsilon_p) - (1-f)\frac{\varepsilon_p}{2}\int_{-1}^{1} \frac{g_m(x)}{\tau + x} dx. \tag{8}$$

However, the spectral representation functions $g_p(x)$ and $g_m(x)$ are not independent since they are correlated through the expression (according to the Fuchs and Claro notation[14])

$$(1-f)ng_m(n) = f(1-n)g_p(1-n), \tag{9}$$

which, after introducing the change of variable [Eq. (4)], transforms into

$$(1-f)\frac{1-x}{2}g_m(x) = f\frac{1+x}{2}g_p(-x). \tag{10}$$

However, there is an alternative way to describe the spectral density function without ambiguity of media. This can be done by taking into account the relationship between g_p and g_m [expressions (9) and (11)] so that we can redefine the two spectral density functions (according to the Fuchs and Claro notation[14]) as follows:

$$\chi_p(n) = \frac{g_p(n)}{(n-1)}, \quad \chi_m(n) = \frac{g_m(n)}{(n-1)}, \tag{11}$$

or in terms of the variable x

$$\chi_p(x) = \frac{2g_p(x)}{(x+1)}, \quad \chi_m(x) = \frac{2g_m(x)}{(x+1)}. \tag{12}$$

Then, the original Eq. (9) from Ref. 14, (11), can be rewritten as

$$(1-f)\chi_m(-x) = f\chi_p(x). \tag{13}$$

It results that the spectral function χ_p times its filling factor is related with the corresponding function χ_m by just an inversion of variable. Thus, the effective dielectric constant can now be calculated by using

$$\langle\varepsilon\rangle = \varepsilon_m + fC_p(\varepsilon_p - \varepsilon_m) + \frac{f\varepsilon_m}{2}\int_{-1}^{1} \chi_p(x)\frac{x+1}{\tau - x} dx \tag{14}$$

or

$$\langle \varepsilon \rangle = \varepsilon_m + fC_p(\varepsilon_p - \varepsilon_m) + f\varepsilon_m \left[\frac{(\tau+1)}{2} \int_{-1}^{1} \frac{\chi_p(x)}{\tau - x} dx - \frac{1}{2} \int_{-1}^{1} \chi_p(x) dx \right]. \tag{15}$$

Introducing the sum rules that link the percolation strengths with the spectral representation functions (according to the Fuchs and Claro notation[14]), we end up having

$$(1-f)C_m + fC_p + f \int_0^1 \frac{g_p(n)}{1-n} dn = 1, \tag{16}$$

$$(1-f)C_m + fC_p + (1-f) \int_0^1 \frac{g_m(n)}{1-n} dn = 1; \tag{17}$$

these equations transform into the expressions below after introducing the change of variables from g, n to χ, x [Eqs. (4) and (5)],

$$(1-f)C_m + fC_p + \frac{f}{2} \int_{-1}^{1} \chi_p(x) dx = 1, \tag{18}$$

$$(1-f)C_m + fC_p + \frac{(1-f)}{2} \int_{-1}^{1} \chi_m(x) dx = 1. \tag{19}$$

Finally, introducing Eq. (18) into (15), we have obtained a unified expression both for m and p media,

$$\langle \varepsilon \rangle = f\varepsilon_p C_p + (1-f)C_m\varepsilon_m + 2f \frac{\varepsilon_p \varepsilon_m}{\varepsilon_p - \varepsilon_m} \int_{-1}^{1} \frac{\chi_p(x)}{\tau - x} dx. \tag{20}$$

This expression combines the information of both spectral representation functions into a single one. The use of a unified expression enhances the precision degree because, it can be seen that if the spectral representation functions are deduced from experimental data by separately using Eqs. (7) and (8), the resulting $g_p(n)$ and $g_m(n)$ do not satisfy Eq. (9) because large errors appear for values of n close to 1 in both cases. Thus, the use of both functions allows one to get precise values for $g_p(n)$ for values of n ranging from 0 to 0.5, while the use of $g_m(n)$ to determine $g_p(n)$ through Eq. (9) allows one to estimate this function in an interval of n ranging from 0.5 to 1. It should be pointed out that Day *et al.*[24] were aware of this fact but they used a linear combination of these two functions instead of a unified expression.

It is possible to expand the spectral density function, χ_p, as an infinite series of orthogonal functions. We have chosen the Legendre polynomials[28,29] since they are the natural orthogonal polynomials along the interval $[-1,1]$ in order to use the Gaussian quadrature formula to estimate the integrals. Thus, we can write $\chi_p(x)$ as

$$\chi_p(x) = \sum_{k=0}^{\infty} \gamma_{pk} P_k(x). \tag{21}$$

In the case that the spectral representation functions were known, the expansion coefficients could be calculated by

$$\gamma_{pk} = \frac{2k+1}{2} \int_{-1}^{1} \chi_p(x) P_k(x) dx; \tag{22}$$

considering expression (21), we can now rewrite Eq. (20) as

$$\langle \varepsilon \rangle = f\varepsilon_p C_p + (1-f)C_m\varepsilon_m + 2f \frac{\varepsilon_p \varepsilon_m}{\varepsilon_p - \varepsilon_m} \sum_{k=0}^{\infty} \gamma_{pk} Q_k(\tau), \tag{23}$$

where the Q_k's are the Legendre functions of the second kind, which are the Hilbert transformation of the P_k's Legendre polynomials. It is important to note that the Q_k functions can be easily estimated. In the case of the first terms they can be calculated analytically in a straightforward way (see the Appendix). The analyticity of the Hilbert transform of the Legendre polynomials is another reason to justify the selection of this base. Although any of the Q_k terms can be recursively obtained, in the case of higher orders (from the sixth and higher) the numerical errors produced in the evaluation of the explicit expressions become unacceptable so that we have used the numerical procedure introduced by Gil and Segura.[30] The same expansion can be applied to $\chi_m(x)$. According to expression (13), the coefficients γ_{mk} and γ_{pk} are related through the expression

$$\gamma_{mk} = \frac{(-1)^k f}{1-f} \gamma_{pk}. \tag{24}$$

At this point, it is convenient to introduce the sum rules for the spectral functions χ_p and χ_m as (according to the Fuchs and Claro notation[14])

$$\int_0^1 g_p(n) dn = 1 - C_p,$$

$$\int_0^1 g_m(n) dn = 1 - C_m, \tag{25}$$

which transforms into the following equations by introducing the x variable and Eqs. (11), (12), and (21),

$$\frac{1}{2} \int_{-1}^{1} g_p(x) dx = \frac{1}{4} \sum_{k=0}^{\infty} \gamma_{pk} \int_{-1}^{1} (1+x) P_k(x) dx = 1 - C_p \tag{26}$$

and

$$\frac{1}{2} \int_{-1}^{1} g_m(x) dx = \frac{1}{4} \sum_{k=0}^{\infty} \gamma_{mk} \int_{-1}^{1} (1+x) P_k(x) dx = 1 - C_m. \tag{27}$$

Operating on expressions (24)–(27), we obtain the following set of equations for the first two terms of the expansion,

$$\frac{\gamma_{p0}}{2} + \frac{\gamma_{p1}}{6} = 1 - C_p,$$

$$\frac{\gamma_{m0}}{2} + \frac{\gamma_{m1}}{6} = 1 - C_m, \tag{28}$$

which results in

$$f\gamma_{p0} = f(1 - C_p) + (1 - f)(1 - C_m), \tag{29}$$

$$\frac{f\gamma_{p1}}{3} = f(1 - C_p) - (1 - f)(1 - C_m). \tag{30}$$

Introducing the variable x, the second sum rule [expression (26)] becomes

$$\frac{1}{8}\int_{-1}^{1}(1 - x^2)\chi_p(x)dx = \frac{1}{3}(1 - f). \tag{31}$$

Expanding $(1-x^2)$ and $\chi_p(x)$ in their Legendre polynomials series, it results that

$$\gamma_{p0} - \frac{\gamma_{p2}}{5} = 2(1 - f). \tag{32}$$

As a result, we have that the first three Legendre coefficients of the effective dielectric constant given by Eq. (22) are correlated and depend on the percolation strengths C_p and C_m. The explicit expressions for the first three coefficients are

$$\gamma_{p0} = -C_p + \frac{1}{f}[1 - (1 - f)C_m],$$

$$\gamma_{p1} = 6 - 3C_p - \frac{3}{f}[1 - (1 - f)C_m],$$

$$\gamma_{p2} = -10(1 - f) - 5C_p + \frac{5}{f}[1 - (1 - f)C_m]. \tag{33}$$

Therefore, collecting all the terms, Eq. (23) can be rewritten in the following compact form:

$$\langle\varepsilon\rangle = fC_p\varepsilon_p\Phi_p(\tau) + (1 - f)C_m\varepsilon_m\Phi_m(\tau) + 2f\frac{\varepsilon_p\varepsilon_m}{\varepsilon_p - \varepsilon_m}\left[\Phi_0(\tau) + \sum_{k=3}^{\infty}\gamma_{pk}Q_k(\tau)\right], \tag{34}$$

where

$$\Phi_p(\tau) = 1 - (\tau - 1)[Q_0(\tau) - 3Q_1(\tau) + 5Q_2(\tau)], \tag{35}$$

$$\Phi_m(\tau) = 1 - (\tau + 1)[Q_0(\tau) + 3Q_1(\tau) + 5Q_2(\tau)], \tag{36}$$

$$\Phi_0(\tau) = [Q_0(\tau) - 3(2f - 1)Q_1(\tau) + 5(1 - 2f + 2f^2)Q_2(\tau)]. \tag{37}$$

It is important to remark that Eq. (34) allows to calculate the effective dielectric constant in a fully analytical way, avoiding numerical integration required for the calculation of the Hilbert transform. Moreover, the sum rules are implicitly included in this equation, so that no further check of the validity of the solution referring to these constraints are required. Finally, it will be shown later that, even if the summation term is dropped from expression (34), it still produces an acceptable approximation to the effective dielectric constant.

III. EXPERIMENTAL PROCEDURE

Pressed pellets of MgO and NaF were obtained by compressing submicrometric powders under 800 MPa and vacuum with a smooth die of YTZP (yttria/tetragonal zirconia partially stabilized). The resulting pellets had a roughness much smaller than the infrared wavelengths considered in the experiment. Additionally, KBr/CaF_2 composites with volume concentrations of 0.03, 0.15, 0.20, and 0.3 of calcium fluoride were prepared by solving KBr in de-ionized water, and then adding submicrometric powder of CaF_2 to prepare a suspension (CaF_2 is poorly soluble into water). The suspension was continuously stirred until the KBr precipitated and dried for 8 h under agitation in order to prevent the CaF_2 segregation. Only fluorite concentrations below 30% were prepared to avoid porosity. The resulting powder were pressed in the same way as the MgO and NaF pellets. Measurements of the IR reflectance at near normal incidence (12°) were performed with a specular reflectance attachment in a Bruker 66V/S FTIR (Fourier transform infrared) spectrophotometer with CsI ($1000-250\ cm^{-1}$) and Mylar® 50 μm ($400-50\ cm^{-1}$) beam splitters and their corresponding deuterated triglycine sulfate (DTGS) detectors.

IV. EXPERIMENTAL RESULTS

In order to check the proficiency of the present method to extract the spectral density function from specular normal incidence reflectance experiments, several spectra corresponding to heterogeneous materials have been recorded. Particularly, two types of composites have been chosen: (a) single component porous pellets and (b) mixtures of alkaline halides. In the case of porous pellets, special care was taken to obtain surface roughness and volume porosity much smaller than the incident infrared wavelength (equal or less than 1 μm). However, the correct preparation of mixtures of different materials requires the removal of porosity (air) while maintaining a good homogeneity. The conditions that induce composite heterogeneity occur when the powdered material is formed by particles of different sizes or when one of the constituents suffers an anomalous grain growth driven to coalescence to the second component. Under these circumstances, the grain size of one or both components of the composite becomes comparable or larger than the IR wavelength so that the quasistatic approximation is no longer valid, and some different model must be introduced to reproduce the experimental reflectance spectrum.

A. Porous ionic pellets

Two different ionic substances have been chosen to prepare the pellets, most of which have a different microstructure. The systems considered are NaF and MgO. In the first material,[31] the main transverse phonon is located at around $250\ cm^{-1}$. As most of halides, this material sinters under pressure at room temperature, so pellets of high concentra-

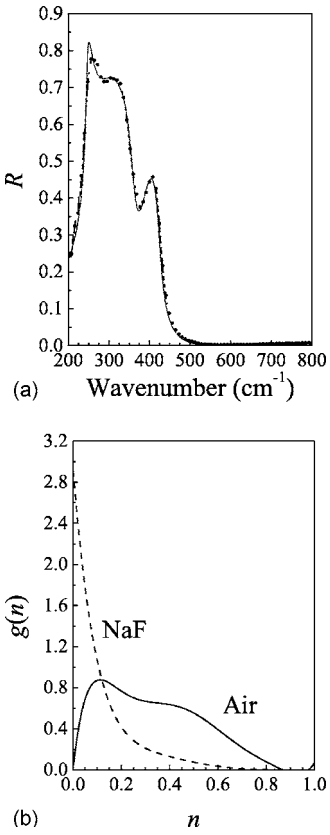

FIG. 1. (a) Experimental near normal reflectance spectrum (dotted line) for NaF/air (with $f_{NaF}=0.88$) and the corresponding fit (solid line) according to the present model. (b) Spectral density functions for NaF and air.

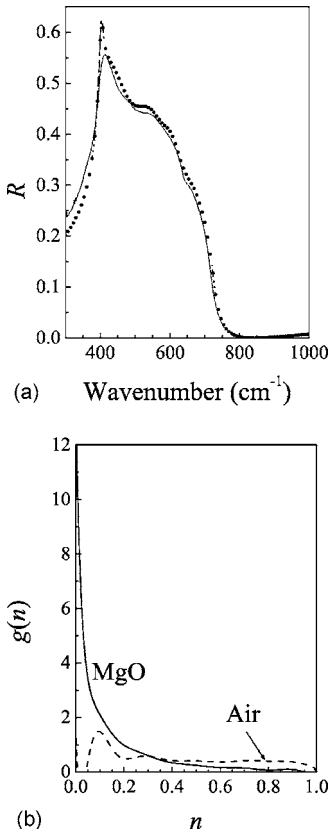

FIG. 2. (a) Experimental near normal reflectance spectrum (dotted line) for MgO/air (with $f_{MgO}=0.60$) and the corresponding fit (solid line) according to the present model. (b) Spectral density functions for MgO and air.

tion were obtained ($f=0.88$). The second type of compound, MgO, is a strongly ionic oxide with very large values of the dielectric constant at the reststrahlung frequency,[32] located at 401 cm^{-1}. As for the case of NaF, MgO has a salt rock crystalline structure, with only one main IR mode (plus a weak secondary one).

The experimental IR reflectance and the corresponding fits provided by the model for NaF/Air and MgO/Air are represented in Figs. 1(a) and 2(a), respectively.

The fit to the experimental reflectance curve of NaF/Air was remarkably good with only six terms. The spectral density function is shown in Fig. 1(b) for air and NaF.

In the case of the MgO/Air sample, only a modest compaction degree ($f=0.62$) could be achieved. The corresponding reflectance spectrum appears in Fig. 2(a) while the spectral density function (fitted with 12 coefficients) is presented in Fig. 2(b).

B. Binary insulator mixtures

The design and preparation of ideal binary mixtures suitable to be studied by IR spectroscopy in order to check the proposed model is not a simple task. For the sake of simplicity, two isotropic compounds with nonoverlapping reststrahlung frequencies are desirable. Moreover, the composite must be dense and, in addition, the particle sizes must be much smaller than the incident wavelength. These two latter conditions impose the condition of absence of porosity and coalescence phenomena. While porosity introduces a new phase (air) in the composite, coalescence causes the growth of some of the component grains to sizes larger than the IR wavelength. Therefore, the quasistatic approximation ($2\pi n/\lambda \ll a$, where a is the average size of a single particle and n is its refractive index) would no longer be valid, and scattering and retardation effects should be taken into account.

Therefore, we choose two plastic phases (halides), KBr/CaF_2, with similar grain sizes and similar growth rates to prepare the composites. The reflectance of a pressed powder pellet of KBr/CaF_2 is shown in Fig. 3(a). We see from this figure that, in the case of very low CaF_2 concentration ($f=0.03$), the reflectance peak is around 258 cm^{-1}, that is, at higher frequency than the transverse CaF_2 phonon.[33] It indicates that this composition is below the percolation threshold [see Fig. 3(b)]. Additionally, the spectral density functions of these spectra are shown in Fig. 3(c), where it can be observed how the spectral density function corresponding to composites with the lowest concentration ($f=0.03$) exhibits a maximum around $n=1/3$, which is in good agreement with all the effective medium theory limits. On the contrary, spectra of higher concentrations present a definite maximum very close to the fluorite transverse phonon frequency. The fit

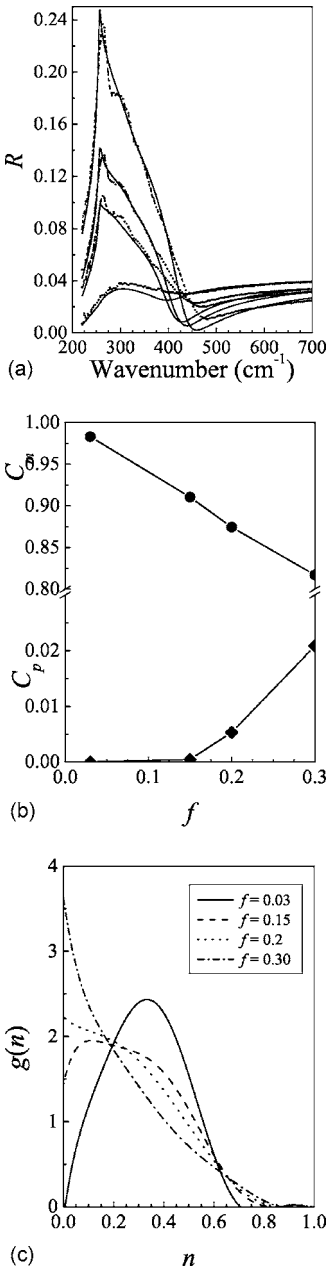

FIG. 3. (a) Experimental near normal reflectance spectra (dotted lines) for the composite KBr/CaF_2 and the corresponding fits (solid lines) according to the present model for f_{CaF_2} ranging from 3% (lower curves) to 30% (upper curves). (b) Percolation strengths of phases KBr and CaF_2 for f_{CaF_2} ranging from 3% to 30%. (c) Spectral density functions for the composite KBr/CaF_2 for f_{CaF_2} ranging from 3% to 30%.

assumes that calcium fluoride is percolated and their spectral representation function presents large values for $n=0$.

V. DISCUSSION

We consider that the present approach is simpler than the ones previously mentioned in the sense that, in many cases, an accurate spectral density function can be derived analytically as the sum of only the first three terms of an expansion of $g(n)$ on Legendre polynomials. An additional advantage of the present work is that it describes the spectral density function without ambiguity of the composite phases (either p or m) chosen to calculate the spectral density function. Therefore, the effective dielectric constant of the composite is independent of the choice of matrix (m) and inclusion (p), as Eq. (23) indicates. Moreover, this effective dielectric constant can be calculated analytically. In fact, only logarithm and polynomic functions are needed to calculate $\langle\varepsilon\rangle$.

The main difference of the present formalism, with respect to previous ones,[22,24] is the expansion of the spectral representation function as a linear combination of elements of an orthonormal base. This base is defined by the scalar dot product defined in the space of continuum functions in the interval of $x \in [-1,1]$,

$$(f \cdot g) = \int_{-1}^{1} w(x) f(x) g(x) dx. \tag{38}$$

This formalism implies that, even after the truncation of the series, the approach remains optimal. Thus, the degree of the precision attained and the simplicity of the calculations only depend on the chosen basis and on the order of the expansion. In fact, the simpler base is a constant sampling of $\chi_p(x)$ along $[-1,1]$ in N intervals that can be written as[22,24]

$$\phi_k = \sqrt{\frac{N}{2}}[\theta(x - x_{k-1}) - \theta(x - x_k)], \tag{39}$$

where $\theta(x)$ is the step function, k runs from 1 to N, and $x_k = -1 + 2(k/N)$. In this sense, the reduced spectral density functions $\chi_p(x)$ and $\chi_m(x)$ can be written as

$$\chi_p(x) = \sum_{k=1}^{N} t_{p,k} \phi_k(x),$$

$$\chi_m(x) = \sum_{k=1}^{N} t_{m,k} \phi_k(x), \tag{40}$$

where the coefficients $t_{p,k}$ and $t_{m,k}$ are the mean values of spectral representation functions, $\chi_p(x)$ and $\chi_m(x)$, along the interval $[x_{k-1}, x_k]$. Their explicit expressions are

$$t_{p,k} = \sqrt{\frac{2}{N}} \int_{x_{k-1}}^{x_k} \chi_p(x) dx,$$

$$t_{m,k} = \sqrt{\frac{2}{N}} \int_{x_{k-1}}^{x_k} \chi_m(x) dx. \tag{41}$$

According to Eq. (13), it can be seen that coefficients $t_{p,k}$ and $t_{m,k}$ are related through

$$f t_{p,k} = (1 - f) t_{m,N-k+1}. \tag{42}$$

Finally, the effective dielectric constant can be estimated as follows:

$$\langle \varepsilon \rangle = f\varepsilon_p C_p + (1-f)C_m\varepsilon_m + 2f\frac{\varepsilon_p\varepsilon_m}{\varepsilon_p - \varepsilon_m}\sum_{k=1}^{N} t_{p,k}L_k(\tau), \tag{43}$$

where C_m, C_p, and t_{pk} will be the fitting parameters, and the function $L_k(\tau)$ is defined by

$$L_k(\tau) = \sqrt{\frac{N}{2}}\int_{x_{k-1}}^{x_k}\frac{1}{\tau - x}dx = \sqrt{\frac{N}{2}}\ln\left[1 - \frac{2}{(\tau+1)N - 2k}\right]. \tag{44}$$

The main difference of this approach, similar to that postulated in Refs. 22 and 24, with respect to that of the present article [expansion of $\chi_p(x)$ as Legendre polynomials], is that, in the present approach, the sum rules are used to determine the value of the first three coefficients as a function of the percolation strengths, while for interval based expansions, as those of Refs. 22, 24, and 28, the sum rules must be introduced through equations as constraints that considerably complicate the application of this procedure. In fact, the explicit expression of the first sum rules for $\chi_p(x)$ can be written as

$$\int_0^1 g_p(n)dn = 1 - C_p,$$

$$\int_0^1 g_m(n)dn = 1 - C_m, \tag{45}$$

$$\frac{f}{N}\sqrt{\frac{2}{N}}\sum_{k=1}^{N} t_{p,k} = fC_p + (1-f)(1-C_m). \tag{46}$$

The same expansion may be done by choosing some different bases, such as trigonometric functions, in which case the coefficients to be fitted should be related to the Fourier transform of the spectral representation function. However, to the best of our knowledge, we think that the Legendre polynomial expansion is the most advantageous in order to simplify the calculation.

In fact, it is possible to directly generate a spectral density function just by truncating the Legendre polynomial expansion of $\chi_p(x)$ at the second term, in such a way that the coefficients are solely determined by C_p and C_m. This approximation is similar to that employed in Ref. 9. In this work, an effective medium approximation was introduced to describe the dielectric constant of the experimental powder compact. This approximation has become a valuable tool to determine IR optical constants of materials that cannot be obtained as single crystals.[34,35] This method has been applied to some of the most employed substances in the world of material science [for instance, ceramic such as t-ZrO_2 (Ref. 36) or transitional aluminas, magnetic materials, γ-Fe_2O_3,[37] or ion conductors such as[38] $Li_{4/3}Ti_{5/3}O_4$]. The most remarkable feature of the work of Ref. 9 is that the most relevant microstructural parameters resulted to be the percolation threshold (which is related to particle and matrix shapes) or, more specifically, the volume concentration in excess of this magnitude, namely $(f-f_c)$. It should be noted that, according to the effective medium approximation, this term is proportional to C_m. In the following, we will discuss the validity of a simple effective medium approximation in which the only fitting parameters will be the percolations strengths.

According to our tests, for composites with intermediate concentrations, reasonable fits can be obtained for the spectral density function to a third degree polynomial. However, due to the smooth profile of a third degree polynomial, it is expected that this approximation may fail for highly diluted systems $(f<0.01)$. Moreover, under these conditions, an analytic expansion of the spectral representation functions is possible. In fact, for a low concentration of the p component, the percolation strengths, C_p and C_m, can be written as

$$\lim_{f\to 0} C_p = 0,$$

$$\lim_{f\to 0} C_m = 1 + \left.\frac{dC_m}{df}\right|_{f=0} f. \tag{47}$$

According to these assumptions, the first three coefficients of $\chi_p(x)$ can be written as

$$\gamma_{p0} = 1 - \frac{dC_m}{df},$$

$$\gamma_{p1} = 3\left(1 + \frac{dC_m}{df}\right),$$

$$\gamma_{p2} = -5\left(1 + \frac{dC_m}{df}\right), \tag{48}$$

so that the reduced spectral function can be written as

$$\chi_p(x) = \frac{7}{2} + \frac{3}{2}\frac{dC_m}{df} + \left(1 + \frac{dC_m}{df}\right)\left(3x - \frac{15}{2}x^2\right). \tag{49}$$

In order to fulfill the positive definite condition for $\chi_p(x)$, the variation of the percolation strength at $f=0$ cannot take any value. Expression (49) takes positive values for $-7/9 < (dC_m/df) < -19/9$ (Fig. 4). However, for this range of values, the spectral representation function does not tend to zero for $n=0$ (or $x=1$). In fact, this condition is attained when $(dC_m/df) < -1/3$, so that $\chi_p(x) = -5x^2 + 2x + 3$. The corresponding spectral representation $g_p(x) = 1/2(x+1)(-5x^2+2x+3)$ reaches its maximum at $x = \frac{\sqrt{84}-3}{15} \cong 0.4078$ or $n = 0.2945$, very close to $n=0.3333$, which corresponds to the maximum of a spectral representation function of a diluted suspension of spheres. However, it should be noted that this spectral representation function takes small negative values in a narrow region of x close to 1. Then, it can be concluded that the use of only three terms into the Legendre polynomial expansion of $\chi_p(x)$ could be a very simple, fast, and valuable approximation. However, some caution must be taken into account when considering only C_p and C_m to estimate the full spectral representation function, especially for low concentrations values. Under these circumstances, we recommend the use of some additional terms in order to get more accurate results.

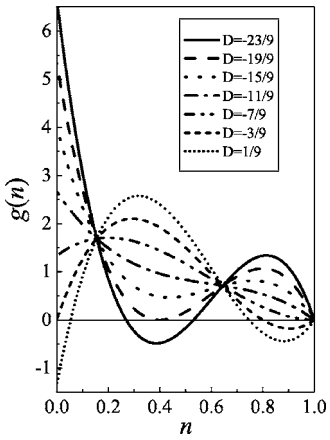

FIG. 4. Spectral density functions in the low concentration approximation, considering only C_p and C_m as the fitting parameters. Several curves are shown for different values of $D=dC_m/df$.

The fitting of the experimental reflectance spectra of NaF/air, MgO/air, and KBr/CaF_2 composites to the proposed model is, in general, quite remarkable. As a result of the fitting, it is possible to obtain the experimental shape of the spectral representation functions for the studied systems. In the case of the dielectric/air composites [Figs. 1(b) and 2(b)], the spectral representation functions of the dielectric, labeled $g_p(n)$, present a pronounced increase for n approaching zero.[39] This behavior corresponds to a percolated phase. Moreover, this curve present a close resemblance to the model reported by Poladian[40] for periodic arrays of touching spheres. The spectral representation functions of air, designated as $g_m(n)$, exhibit definite maxima at $n=0.11$ and $n=0.45$ for the NaF/air system [Fig. 1(b)], and at $n=0.09$ and $n=0.30$ for the MgO/air composite [Fig. 2(b)]. These values of n correspond to pores with oblate shapes.

With regard to the KBr/CaF_2 composite, we see in Fig. 3(a) that the maximum corresponding to the lowest CaF_2 concentration sample ($f=0.03$) appears at around 300 cm^{-1} [Fig. 3(a)]. Moreover, the minimum of the reflectance is nearly missing. The latter is the behavior of a nonpercolated material as seen in Fig. 3(b). The spectral representation function of this sample shows a maximum at $n=0.33$, which corresponds to disperse spherical particles. However, this maximum is not as sharp as it should be considering the low concentration of the sample. This suggests that fluorite particles suffer some large degree of agglomeration in spite of the precautions taken to prepare the composite. This behavior can be clearer observed in the rest of the samples of the series since they are all percolated [see Fig. 3(b)]. As the CaF_2 concentration increases, the sharp maxima of the reflectance appear at the transverse phonon wave number (270 cm^{-1}) and the minima shift toward higher wave numbers [see Fig. 3(a)].

The spectral representation functions of the KBr/CaF_2 evolve from a single peaked function ($f=0.03$) to a function with a pronounced increase for n approaching zero ($f=0.30$) going through a double headed function ($f=0.15$) in the neighborhood of the percolation threshold. As can be seen in Fig. 3(c), the derived spectral representation functions follow the behavior that can be expected for composites with concentrations in the surrounding area of the percolation threshold.

It is worth mentioning the sensitivity of the method in order to determine the position of the maxima and minima for concentrations close to the percolation threshold. The reason underlying the above mentioned sensitivity has to do with the behavior of the second kind Legendre functions, $Q_k(\tau)$. These functions exhibit two singularities at $\tau=\pm 1$, which correspond to the transverse (ω_T) and longitudinal (ω_L) frequencies of the phonon, respectively. Moreover, the frequency associated with the reflectance minimum, ω_m, fulfills the condition $\varepsilon_p(\omega_m)=\varepsilon_m(\omega_m)$ at $\tau=\infty$, where $Q_k(\infty)=0$. Thus, it can be inferred that, in a relatively narrow spectral region from ω_T to ω_m, the real part of the second kind Legendre functions takes all the possible values of the real axis. The latter allows to univocally determine the coefficients of the spectral representation function in the bases of the Legendre polynomials.

According to our experience, the main drawback of the proposed method in this paper is the fact that negative values of the spectral representation function are often obtained for some values of n. The latter statement always applies when particle aggregation phenomena have been detected (by electron and/or optical microscopy). In this regard, it is worth mentioning that the creation of a perfectly dispersed (shuffled) composite is quite difficult due to the interaction forces of the particle surfaces and their low size. As a consequence of this, it is usual to find large clusters (>1 μm) formed of submicrometer-sized particles. In order to determine the effect of clusters comparable to or larger than the wavelength on the effective refractive index, several theoretical models have been proposed.[41–44] Although the range of application of these models, referring to the particle size, is limited, all of them show a notable variation in the effective properties. Moreover, the experimental effective refractive index of composites made by large particles can be outside of both the Hashin-Strickman and Wiener bounds.[44,45] In this regard, it can be concluded that negative values in some spectral representation functions are not due to a flaw of the proposed method but to scattering phenomena produced by large clusters. Therefore, special care must be taken when preparing composites free of agglomerates in order to keep the quasistatic approximation ($k=2\pi n/\lambda$, wave vector, much larger than a, the particle sizes). In the case of moderate agglomeration ($a\sim k/10$), scattering effects, although present, can be neglected so that we succeed to eliminate them by applying the constriction of positive defined $g(n)$ to the least square fitting. Once more, the choice of the Legendre polynomials allows one to notably simplify the introduction of the above mentioned constriction. Thus, we have introduced linear inequalities assuming two type of conditions,

$$0 \leq C_p \leq 1, \quad 0 \leq C_m \leq 1, \tag{50}$$

and

$$\chi_p(x_l) = \sum_{k=0}^{N} \gamma_{pk} P_k(x_l) \geq 0, \tag{51}$$

where x_l are points in the interval $0 \leq x_l \leq 1$. In order to cover a homogeneous range of values of x, we have chosen the zeros of the $P_{k+1}(x)$ Legendre polynomial because they satisfy the condition that they remain unchanged if the summation was truncated at the $k+1$th term instead of at the kth term.

The formalism developed in the present work is, on one hand, of interest for the fundamental knowledge of the electromagnetic properties of heterogeneous materials and, on the other hand, it can be a very useful tool for determining morphological and microstructural properties of materials of technological interest. For example, this procedure, or a generalization of it for anisotropic substances, could be used to determine, among others, the shape and connectivity of pores in dense ceramics, orientation and distribution of fibers in reinforced composites, and the shape and agglomeration state of powdered materials.

VI. CONCLUSIONS

We have developed a relatively simple, reliable, and robust procedure to extract the spectral representation function from experimental infrared near normal reflectance data. For this spectral range, a quasistatic approximation was assumed in order to neglect scattering effects. The ideas underlying the present formalism are, first, the merging of the spectral representation functions corresponding to each of the phases of a binary composite into a single one and, second, the expansion of the latter function in the orthogonal base of a Legendre polynomial.

We have been able to extract the spectral representation function of a series of composites made of different types of materials. The behavior of the obtained functions agree well with some previous theoretical works. However, special care must be taken in the preparation stages in order to avoid agglomeration phenomena, which produce large clusters that break the quasistatic approximation due to scattering effects.

ACKNOWLEDGMENTS

F.J.G-V. acknowledges partial support by CSIC-CAM (under project 200550M016) and C.P. acknowledges the EU IP NANOKER project FP6-515784-2.

APPENDIX: LEGENDRE POLYNOMIALS AND SECOND KIND LEGENDRE FUNCTIONS

Although readers can find the explicit expressions of both Legendre polynomials and function in several handbooks, we think it is pertinent to include here their explicit expressions up to the fifth degree of both functions in order to help readers to implement the explicit calculation of the spectral density function with the present model:

$$P_0(x) = 1,$$

$$P_1(x) = x,$$

$$P_2(x) = \frac{3x^2 - 1}{2},$$

$$P_3(x) = \frac{5x^3 - 3x}{2},$$

$$P_4(x) = \frac{35x^4 - 30x^2 + 3}{8},$$

$$P_5(x) = \frac{63x^5 - 70x^3 + 15x}{8}; \tag{A1}$$

$$Q_0(x) = \frac{1}{2} \ln\left(\frac{1+x}{1-x}\right),$$

$$Q_1(x) = -1 + \frac{x}{2} \ln\left(\frac{1+x}{1-x}\right),$$

$$Q_2(x) = -\frac{3x}{2} + \frac{3x^2 - 1}{4} \ln\left(\frac{1+x}{1-x}\right),$$

$$Q_3(x) = -\frac{15x^2 - 4}{6} + \frac{5x^3 - 3x}{4} \ln\left(\frac{1+x}{1-x}\right),$$

$$Q_4(x) = -\frac{105x^3 - 55x}{24} + \frac{35x^4 - 30x^2 + 3}{16} \ln\left(\frac{1+x}{1-x}\right),$$

$$Q_5(x) = -\frac{945x^4 - 735x^2 + 64}{120} + \frac{63x^5 - 70x^3 + 15x}{16} \ln\left(\frac{1+x}{1-x}\right). \tag{A2}$$

[1] S. Torquato, *Random Heterogeneous Materials* (Springer, Berlin, 2001).

[2] J. D. Jackson, *Classical Electrodynamics* (Wiley, New York, 1962).

[3] J. C. Maxwell-Garnett, Philos. Mag. **203**, 385 (1904); J. C. Maxwell-Garnett, *ibid.* **205**, 237 (1905).

[4] D. A. G. Bruggerman, Ann. Phys. **24**, 636 (1935).

[5] R. Landauer, *Electrical Transport and Optical Properties of Inhomogeneous Media*, AIP Conf. Proc. No. 40 (AIP, New York, 1978), p. 2.

[6] L. D. Landau and E. M. Lifshitz, *Electrodynamics of Continuous Media* (Pergamon, New York, 1984).

[7] R. C. McPhedran and D. R. McKenzie, *Electrical Transport and Optical Properties of Inhomogeneous Media*, AIP Conf. Proc. No. 40 (AIP, New York, 1978), p. 294.
[8] For a revision see V. Ossenkopf, Astron. Astrophys. **251**, 210 (1991).
[9] C. Pecharromán and J. E. Iglesias, Phys. Rev. B **49**, 7137 (1994).
[10] D. Stroud, G. W. Milton, and B. R. De, Phys. Rev. B **34**, 5145 (1986).
[11] D. J. Bergmann, Phys. Rep. **44**, 378 (1978).
[12] R. Fuchs and S. H. Liu, Phys. Rev. B **14**, 5521 (1976).
[13] D. Langbein, J. Phys. A **10**, 1031 (1977).
[14] R. Fuchs and F. Claro, Phys. Rev. B **39**, 3875 (1989).
[15] J. Monecke, J. Phys.: Condens. Matter **6**, 907 (1994).
[16] K. Ghosh and R. Fuchs, Phys. Rev. B **44**, 7330 (1991).
[17] R. Stognienko, T. Henning, and V. Ossenkopf, Astron. Astrophys. **296**, 797 (1995).
[18] J. E. Spanier and I. P. Herman, Phys. Rev. B **61**, 10437 (2000).
[19] O. Hudak, I. Rychetsky, and J. Petzelt, Ferroelectrics **208**, 429 (1998).
[20] H. D. Wanzenbýck, B. Edl-Mizaikoff, G. Friedbacher, M. Grasserbauer, R. Kellner, M. Arntzen, T. Luyven, W. Theiss, and P. Grosse, Mikrochim. Acta **Suppl. 14**, 665 (1997).
[21] A. V. Goncharenko and E. F. Venger, Appl. Phys. A **74**, 649 (2002).
[22] J. Sturm, P. Grosse, and W. Theiss, Z. Phys. B: Condens. Matter **83**, 361 (1991).
[23] E. Gorges, P. Grosse, J. Sturm, and W. Teiss, Z. Phys. B: Condens. Matter **94**, 223 (1994).
[24] A. R. Day, A. R. Grant, A. J. Sievers, and M. F. Thorne, Phys. Rev. Lett. **84**, 1978 (2000).
[25] E. Tuncer, Phys. Rev. B **71**, 012101 (2005).
[26] J. R. Macdonald, J. Chem. Phys. **102**, 6241 (1995).
[27] E. Tuncer, M. Furlani, and B. E. Mellander, J. Appl. Phys. **95**, 3131 (2004).
[28] J. Spannier and K. B. Oldham, *An Atlas of Functions* (Hemisphere, Washington, 1987).
[29] U. W. Hochstrasser, *Handbook of Mathematical Functions*, edited by M. Abramowitz and I. A. Stegun (Dover, New York, 1970), pp. 771–8021.
[30] A. Gil and J. Segura, Comput. Phys. Commun. **105**, 273 (1997).
[31] I. F. Chang and S. S. Mitra, Phys. Rev. B **5**, 4094 (1972).
[32] J. R. Jarperse, A. Kahan, J. N. Plendl, and S. S. Mitra, Phys. Rev. **146**, 526 (1966).
[33] W. Kaiser, W. G. Spitzer, R. H. Kaiser, and L. E. Howarth, Phys. Rev. **127**, 1950 (1962).
[34] C. Pecharromán and J. E. Iglesias, J. Phys.: Condens. Matter **6**, 7125 (1994).
[35] C. Pecharromán and J. E. Iglesias, Appl. Spectrosc. **54**, 634 (2000).
[36] C. Pecharroman, M. Ocaña, and C. J. Serna, J. Appl. Phys. **80**, 3479 (1996).
[37] C. Pecharromán, T. Gonzalez-Carreño, and J. E. Iglesias, Phys. Chem. Miner. **22**, 21 (1995).
[38] C. Pecharromán and J. M. Amarilla, Phys. Rev. B **62**, 12062 (2000).
[39] F. Claro and R. Fuchs, Phys. Rev. B **33**, 7956 (1986).
[40] L. Poladian, Phys. Rev. B **44**, 2092 (1991).
[41] W. Lamb, D. M. Wood, and N. W. Ashcroft, Phys. Rev. B **21**, 2248 (1980).
[42] D. Stroud and F. P. Pan, Phys. Rev. B **17**, 1602 (1978).
[43] A. Wachniewski and H. B. McClung, Phys. Rev. B **33**, 8053 (1986).
[44] D. E. Aspnes, Phys. Rev. B **25**, 1358 (1982).
[45] W. G. Egan and T. Hilgeman, Appl. Opt. **19**, 3724 (1980).